Third-order Nonlinear Dispersion Properties of Surface Plasmon Resonance in Gold Nanoparticles

L. Poperenko, S. Rozouvan*, V. Staschuk

Department of Physics, Taras Shevchenko National University of Kyiv, 4, Glushkov Ave., 03022 Kyiv, Ukraine

Experimental results of degenerate four wave mixing spectroscopy in the visible spectrum for polymer semiconductor films with embedded gold nanoparticles are presented. An enlargement of third-order optical nonlinearity at the shortwave wing of the surface plasmon absorption band was experimentally registered. A theoretical model of surface plasmons as longitudinal standing waves in nano-objects was developed in order to analyze the experimental data. As it was pointed, the amplification of the third-order nonlinear coefficients occurs in the spectral region with simultaneously large numbers of dielectric constant and refractive index. Experiments using scanning tunneling microscopy with a spatial resolution of up to 1 nm allowed us to characterize in detail the morphology of the sample with embedded gold nanoparticles. Microscopy measurements results showed that nanoparticles with a size of 10-20 nanometers have a non-spherical shape and amorphous ordering of atoms. The nanoparticles were found to be coupled into clusters having a few hundred nanometers dimensions. Numerical solutions of Maxwell's equations for nanoparticles having the shape, which was previously experimentally measured by scanning tunneling microscopy, were obtained. The results of the calculations confirm a homogeneous character of the plasmon absorption band spectral broadening in samples and suitability of the developed theoretical approach where spectral properties of surface plasmons can be considered in frames of harmonic damping oscillator model. Degenerate four wave mixing interaction in an organic polymer with embedded gold nanoparticles was found to be a simultaneous manifestation of two processes – quantum mechanical originated third-order nonlinear interaction and a longitudinal standing wave of charge carriers, which can be correctly explained in frames of the classical electrodynamics.

Keywords: Surface plasmon, Gold nanoparticles, Organic semiconductor, Third-order nonlinearity, Scanning tunneling microscopy.

1. INTRODUCTION

Plasmon resonance in metal nanoparticles can be treated as resonant oscillations of electrons in volumes less than wavelength of light which induces the oscillations. The effect attracted huge attention of research groups due to numerous nanoparticles related phenomena such as non-linear optics, optical activity or photothermal effects [1]. The plasmon resonant frequencies can differ depending on multitude of factors – nanoparticles' material, shape, size etc. Theoretical description of plasmon resonance in nanoparticles can be based on a few models which can be interpreted as outcomes of Drude theory of metals or Mie scattering theory [2]. The former approach is based on further development of oscillations in plasma formalism for free electrons in metals with nonzero electrical resistivity. Mie based theories describe nanoparticles light scattering by analyzing nanoparticles and host media dielectric constants. However, such classical electromagnetism approaches have to be further clarified in cases when experimental specifics include quantum mechanical phenomena. We can mention, for example, effects of nanoparticles coupling with sub-nanometer gaps [3], necessity to take into account interband and intraband contributions to dielectric function [4]. Optical nonlinearity of composite organic semiconductor – Au nanoparticles media has to be further clarified too because of definite influence of nanoparticles plasmons on purely quantum mechanical degenerate four-wave mixing

(DFWM) processes [5].

The goal of this article is to study both theoretically and experimentally dispersion of third-order nonlinearity in composite organic semiconductor – Au nanoparticles media. Experimental techniques include high spatial resolution scanning tunneling microscopy (STM) measurements which allow to characterize conducting flat surfaces on atomic resolution scale.

2. THEORETICAL APPROACH

Plasmon is a collective mode of electrons oscillation. Classical plasma frequency can be derived from a simple model of electric force applied to displaced electron gas with respect to the fixed positive ions (Fig. 1a). A charges displacement U (white and black bonds in Fig. 1a) results in electric field rise which tends to restore electric charge distribution to equilibrium. The known formula for plasma frequency $\omega_p = \sqrt{Ne^2/\varepsilon_0 m}$ is derived from the equation of collective oscillation of the undamped electron gas system:

$$Nm\ddot{U} = -N^2 e^2 U/\varepsilon_0, \qquad (1)$$

where N is the charges concentration. This model can be directly applied to a case of a perfect conductor with zero resistance and zero electric field in the volume except surface charges on its surface. Numbers U from Fig. 1a are supposed to be negligibly low comparing to

*sgr@univ.kiev.ua

the sample size. In metal nanoparticles, we have non-zero electric resistance contrary to the idealized model of plasma oscillations. Also nanoparticles skin depth numbers are of the same order of magnitude as tens nanometers nanoparticles dimensions! It means we have to take into account the skin effect in the metallic nanoparticles as a part of surface plasmon resonance modelling.
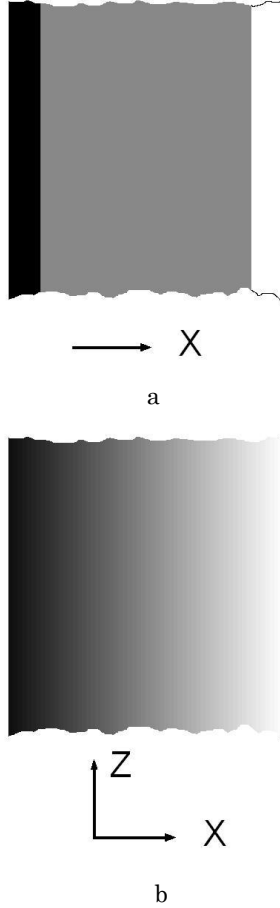

a

b

Fig. 1 – Collective electron oscillation in a) rectangular shaped volume of plasma, b) a metal plate. Gray color scale represents electric charge density: white color – negative charge, gray – neutral, black – positive.

Let us consider a simplified model of electric charge wave in a ten-nanometer-thick metal plate with non-zero electrical resistance (Fig. 1b). A plane light wave propagates along the Z-axis with electric vector being directed along the X-axis. We can write Maxwell equations for electric field distribution inside the plate having orders of magnitude less than the light wavelength:

$$\vec{\nabla} \times \vec{H} = \vec{j} = \sigma \vec{E},$$
$$\vec{\nabla} \times \vec{E} = -\mu_0 \, \partial \vec{H} / \partial t. \qquad (2)$$

Here $\sigma = 2\varepsilon_0 \omega nk$ is the optical conductivity and $n + ik$ is the refractive index. Solving equations (2), we can write an equation for the electric field in the plate with definite boundary conditions:

$$\Delta E = \exp(-i\omega t) \, \partial^2 E_x / \partial x^2 = \mu_0 \sigma \, \partial \left(E_x \exp(-i\omega t) \right) / \partial t =$$
$$= -i\omega\sigma\mu_0 E_x \exp(-i\omega t),$$
$$E_x(0,t) = E_x(d,t) = E_x \exp(-i\omega t). \qquad (3)$$

We presume that in Eq. (3) the values of E_y, E_z, $\partial^2 E_x / \partial z^2$ and $\partial^2 E_x / \partial y^2$ are negligibly small because the plate dimensions in Y and Z directions are larger comparing with the plate width – the most significant electric field variations take place along the plate surface normal. We have an effective electromagnetic wave bending around the plate due to its small dimensions. The second equation in (3) describes the electric field near the plate surface (it has the same numbers there). Solution of Eq. (3) can be written taking into account these boundary conditions:

$$E_x(x,t) = E_0(\exp(-x/\delta) * \exp(-ix/\delta - i\omega t) +$$
$$+ \exp((x-d)/\delta) * \exp(i(x-d)/\delta - i\omega t)) ,$$
$$E_0 = E_x(d) \left[\left(1 + \exp\left(-d/\delta\right) \right) \cos(-d/\delta) \right]^{-1}. \qquad (4)$$

Eqs. (4) describe field distribution inside the plate ($x \in [0; d]$) which may induce standing wave oscillations of the free carriers when $d = \pi\delta j$ ($j = 1, 2, \ldots$). Parameter $\delta = \sqrt{2/(\omega\sigma\mu_0)} = \lambda (2\pi)^{-1} (nk)^{-1/2}$ is the skin depth of electric currents longitudinal flows. Collective motion of the charges exists only in the standing wave fundamental mode when all electrons movement directions are the same at any time moment. Fundamental mode light excitation frequency corresponds to the resonant condition $j = 1$:

$$\omega_{sp} = \frac{\pi c}{d\sqrt{nk}}, \qquad (5)$$

where c is the speed of light. As we can see, Eq. (4) can be interpreted as propagating in the opposite directions two longitudinal decaying waves of electron flows which form a standing wave. The total electric field energy in nano-object for standing resonant wave ($d = \pi\delta$) and off resonant conditions ($d = \pi\delta/2$, $d = 3\pi\delta/2$) reaches one order of magnitude and results in the formation of a single band (surface plasmon band) in the absorption spectrum. Eq. (4) oscillations line width is determined by $d/\delta \in [\pi/2; 3\pi/2]$ wavelength interval. If we have significantly large derivatives $\partial n / \partial \lambda$ and $\partial k / \partial \lambda$ it results in narrower surface plasmon resonance. It correlates with the results from literature – plasmon bands are usually located between interband and intraband transitions spectral regions with large optical constants variations [6].

3. EXPERIMENTAL

We postfabricated gold nanoparticles by annealing procedure because it is a relatively easy and cheap technique allowing to fabricate nanoparticles uniformly deposited on a plane [7]. Gold nanoparticles on a glass substrate were thermally deposited in vacuum. The equipment was directly installed in the vacuum chamber which allowed controlling of the gold temperature, deposition speed and substrate temperature. The substrates which have been used for the film deposition were carefully cleaned and polished glass plates (the roughness was about 0.5 nm). Gold was evaporated onto the slides from a resistively heated tungsten boat. The vacuum chamber was evacuated to a pressure lower than 10^{-5} Torr before the deposition process, and the deposition time interval was selected to fabricate by evaporating the gold film of 10-20 nm thick. The film thickness was precisely controlled afterwards by a profilometer on the edge of the deposited layer. Finally, all the modified substrates were annealed at 450 °C for 1 h on a hot plate in atmospheric air uncontrolled (ambient conditions) when formation of various gold nanoparticles agglomeration was noticed. In order to form samples with third order nonlinear properties, a thin layer of polythiophene derivative (described previously in [8]) was deposited from a solution by doctor blade technique. The solution concentration was chosen to form a polymer layer with small thickness just enough to fill the gaps between nanoparticles agglomerations. It was enough for our purposes to provide interface polythiophene-gold contacts in order to study nanoparticles influenced by the third-order nonlinear signal.

A microscope INTEGRA NT-MDT was used to conduct measurements in scanning tunneling microscopy (STM) regimes. STM spatial resolution reached up to 1.2 nm. A sharp needle for STM measurements was fabricated from 0.5 mm $Pt_{0.8}Ir_{0.2}$ wire by mechanical cutting of its end. We performed our measurements in a regime when STM setup supported a constant tunneling current through the needle, which was accomplished by tuning the sample position along the vertical direction.

The set-up that we used in order to perform spectral DFWM was described in detail in [8]. To perform optical wavelength tuning of femtosecond pulses, a light source consisting of a femtosecond Ti/sapphire oscillator (Coherent Mira 900F), a regenerative Ti/sapphire amplifier (Coherent RegA 9000), and an optical parametric amplifier (OPA) (Coherent 9400) was used. These produced 170 fs pulses were tunable in a wide spectral range, including the wavelength interval from 500 to 700 nm. The repetition rate was 80 kHz, allowing effective lock-in detection in order to improve the signal-to-noise ratio of the DFWM signal in the folded box coherent anti-Stokes Raman scattering (CARS) configuration without generating thermo-optical effects. The three collinear beams (one with a tunable temporal delay) were focused onto the same sample spot by a lens with 100 mm focal length, leading to a focal diameter of approximately 20 μm. The fourth deflected beam as the studied DFWM signal was detected by a silicon photodiode (Hamamatsu followed by a Stanford Research preamplifier SR 620). Lock- in
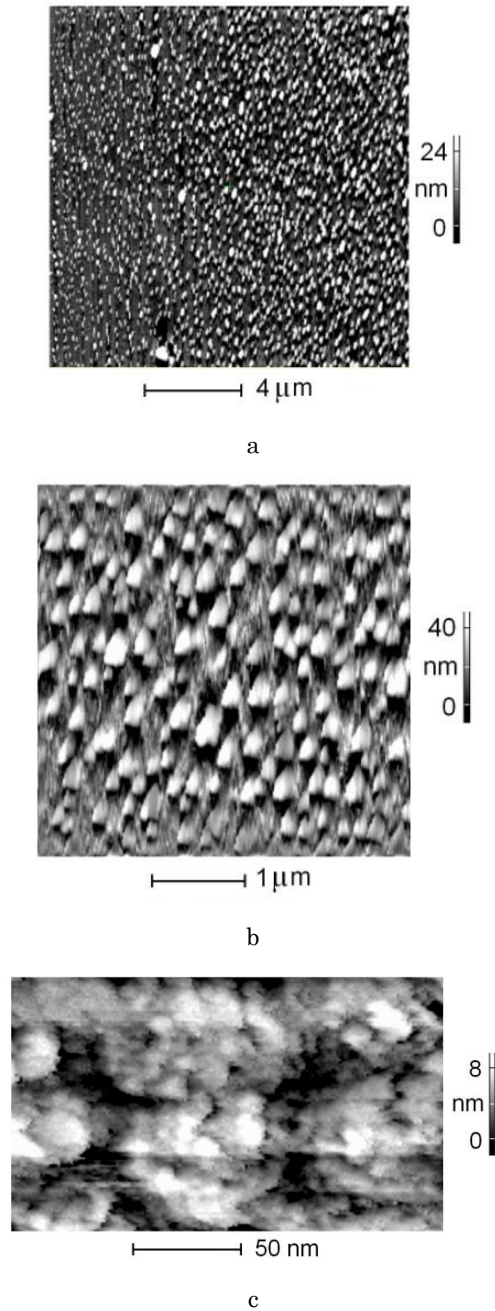
a

b

c

Fig. 2 – STM measurements of nanoparticles agglomerations. Spatial resolution: a) 60 nm, b) 16 nm and c) 1.2 nm

techniques (Stanford Research SR530) were used to improve the signal-to-noise ratio of the DFWM signal. Two of these incoming beams were chopped by a mechanical chopper at different frequencies, and the signal was detected at the frequency sum.

Results of STM measurements with different scan intervals and spatial resolutions are presented in Fig. 2, Fig. 3a. We also performed STM measurements of Au nanoparticles with a few angstroms spatial resolution which revealed amorphous nanoparticles structure. As we can see in the figures, the nanoparticles form clusters uniformly deposited on the surface. STM scans with higher spatial resolution show that the nanoparticles have 10-20 nm sizes with irregular shapes. The nanoparticles form clusters though thin

gaps between single nanoparticles are visible, thus plasmon absorption band originates from 10-20 nm size nanoparticles. In Fig. 4b (curve 3), plasmon band of our sample is homogeneously broadened because of different nanoparticles shapes or/and their sizes variations.

Third-order nonlinear signals at different wavelengths from 508-617 nm spectral interval are presented in Fig. 4a. As we can see, the shapes demonstrate two distinct features. First of all, we can see degradation of coherent artifact (signals maximums in 150 fs of the signals beginning time interval) with reference to slow decay components (signals maximums in the following 150-1000 fs time intervals) as wavelengths enlarge. Also the positions of the signals front slope shift in time to 100-150 fs as wavelengths numbers raise. This behavior of spectral DFWM third-order nonlinear response is similar to the results obtained by us in [5] and seems to be typical for nanoparticles in contact with organic semiconductor. Dispersion curves of absorption and ratio of coherent artifact/slow decay component for current measurements and the results from [5] are presented in Fig. 4. As we discussed earlier, the both curves exhibit drastic drops at surface plasmon bands low energy wings near 520-530 nm. An explanation of these results can be attributed to our standing wave (harmonic oscillator) models.
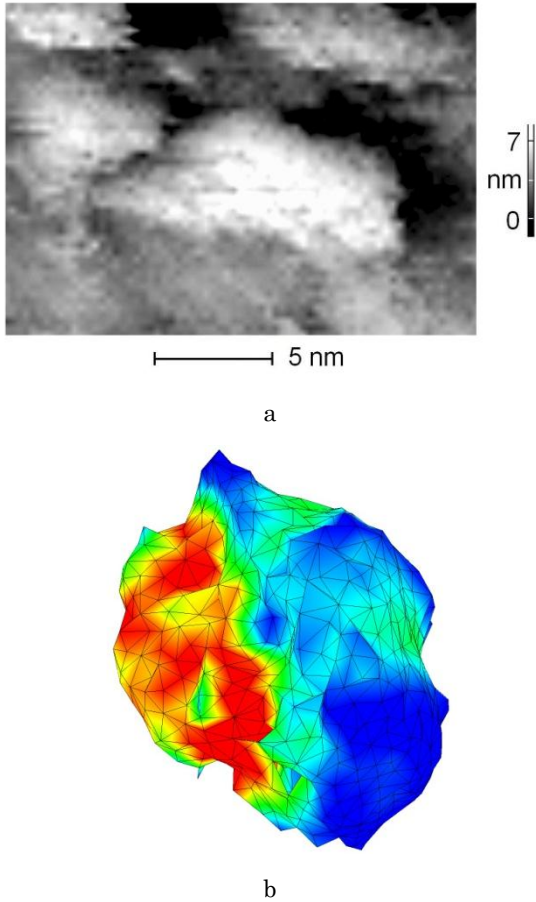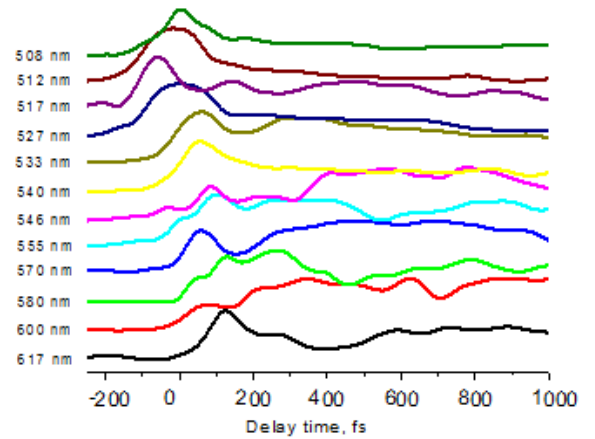
The calculated real part of dielectric permittivity and imaginary part of the refraction index (absorption coefficient) for an idealized harmonic oscillator with damping are presented in Fig. 5. As we can see, extreme numbers of the oscillator dipole moment (minimum of the permittivity curve) are only located in the high-energy wing of the absorption curve similarly to Fig. 4b results. DFWM is a coherent process described by a third-order nonlinear optical tensor which depends on dipole numbers. Linear and third-order nonlinear polarisabilities can be presented as a result of quantum mechanical perturbation theory as [9]:

$$\chi_{ij} = \frac{1}{\hbar} \sum_{i,j=1,2,3} \frac{d_{nm}^{(i)} d_{mn}^{(j)}}{\omega_{mn} - \omega - i\gamma_{mn}}, \qquad (6)$$

$$\chi_{ijkm}^{(3)} = \frac{1}{2\hbar^3} \sum_{i,j,k,m=1,2,3} \left(\frac{d_{nm}^{(i)} d_{ml}^{(j)} d_{lm}^{(k)} d_{mn}^{(m)}}{(\omega_{mn} - \omega - i\gamma_{mn})(\omega_{ln} - \omega - i\gamma_{ln})(\omega_{mn} - \omega - i\gamma_{mn})} + \ldots \right)$$

Here $d_{nm}^{(i)}$ is the dipole moment projection on the *i*-axis as a result of transition between *n* and *m* levels. As we can see, both polarisabilities in frames of quantum mechanical theory depend on dipole moments induced by optical transitions. Therefore, third-order nonlinearities dispersive curve of our sample must be related with dispersive dependencies of dielectric tensor. In turn, absorption curves describe dispersion properties of the refractive index which is a factor in the equation for optical conductivity (introduced in classical electromagnetic theory). As we can see, absorption numbers are simultaneously related to optical nonlinearity enhancement. Thus high third-order nonlinearity in an organic polymer with gold nanoparticles takes place at wavelengths which are determined by simultaneous correlation of both dielectric function and refractive index extrema. From a qualitative point of view, third order nonlinearity enhancement in plasmon band region is a result of quantum mechanical coherent DFWM and classical electrodynamic based collective electron oscillation. As a consequence of this, in Fig. 4b (curves 2 and 4), maximums are asymmetrically located at high energy wing of the sample absorption band with correspondingly large numbers of its refractive index and dielectric function.
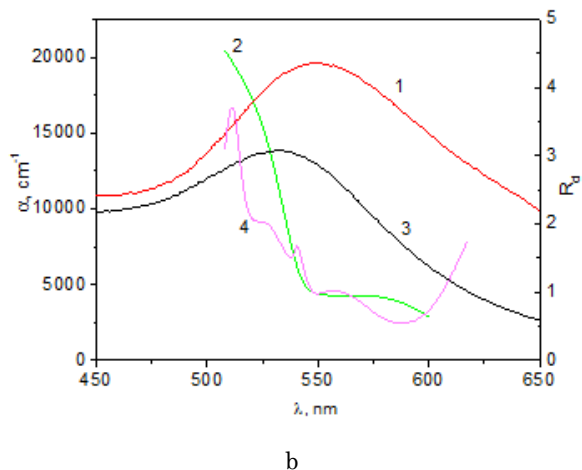

a

b

Fig. 3 – (a) STM measurements of single nanoparticles. Spatial resolution is 0.3 nm. (b) Calculated surface currents at resonant frequency of a nanoparticle from Fig. 3a

a

b

Fig. 4 – (a) DFWM signals at different wavelengths of nanoparticles embedded in polythiophene matrix, (b) 1 – absorption curves and 2 – ratio of coherent artifact/slow decay component for [5] results and for our samples of Au nanoparticles in polythiophene matrix (curves 3 and 4)
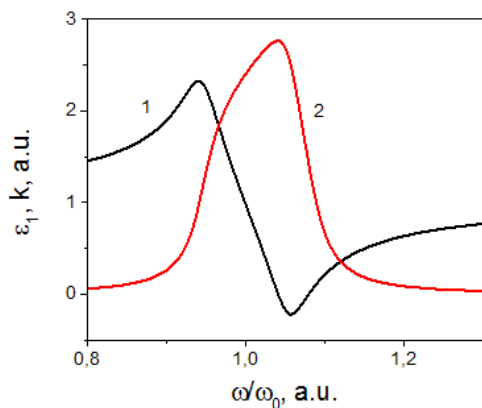

Fig. 5 – Calculated real part of the relative permittivity (1) and imaginary part of the refraction index (2) for harmonic oscillators with damping coefficient $25/\omega_0$

We performed numerical simulation of Maxwell's equation solution for Au nanoparticles. A typical calculations result is presented in Fig. 3b. We modeled a nanoparticle shape taken from Fig. 3a. At first, we built a triangular mesh of the nanoparticle's surface (Fig. 3b) and then numerically solved Maxwell equations for a plane light wave interacting with the surface mesh. A distribution of induced surface currents in colored scale is presented in Fig. 3b. We can see that the distribution forms a dipole. Calculated resonant frequencies for Fig. 2b nanoparticle give 19 % margin

of the relative frequencies differences. It means that Fig. 4b absorption curves may be homogenously broadened due to nanoparticles nonspherical shapes.

As we can see, surface plasmons in gold nanoparticles enhance third order nonlinearity in neighboring polymer. A possible exclusively quantum mechanical theory of optical nonlinearities in composite materials could be based on construction of a mixed state $C_1\psi_{polymer} + C_2\psi_{nanoparticle}$ in the polymer-Au interface layer which would determine the final ground-to-excited state transition dipole moment. Such an approach would require further development of quantum mechanical perturbation theory with surface plasmon modelling as its part.

4. CONCLUSIONS

Plasmon bands in nanoparticles can be represented in a model of a longitudinal standing wave of electric charges. Similarly to "classic" plasma oscillations in a volume of electron gas and positive ions we consider free electrons in a metal plate with nonzero electric resistance. Spectral characteristics of surface plasmon band (bands width/ spectral position etc.) are determined by optical conductivity (or refractive index) parameters and most often are associated with a spectral interval between efficient intraband and interband transitions. A classical electromagnetic theory model can be applied to analyze spectral femtosecond third-order nonlinearity data in organic semiconductors with embedded Au nanoparticles.

Spectral dependent DFWM measurements of nanoparticles embedded in a polythiophene derivative thin film revealed relative enhancement of third-order nonlinearity in high-energy wing of plasmon absorption band. The effect can be explained in frames of simultaneous application of both classical harmonic oscillator and quantum mechanical perturbation theory models. In frames of this model, high-energy wing of the absorption band is associated with higher induced dipole moments and simultaneous high refractive index (optical conductivity) numbers which are responsible for surface plasmon oscillation.

Precise STM measurements with spatial resolution up to 1 nm allowed us to characterize morphology of Au nanoparticles in a polymer matrix. The nanoparticles with 10-20 nm size and nonspherical shapes were found to form 60 nm to 200 nm clusters. Performed numerical solution of Maxwell equations for STM data nanoparticles confirmed possible homogenous broadening of surface plasmon bands in correspondence with the developed theory and performed experiments.

REFERENCES

1. V. Amendola, R. Pilot, M. Frasconi, O.M. Marago, M.A. Iati, *J. Phys. Cond. Mater.* **29** No 20 (2017).
2. A. Moores, F. Goettmann, *New J. Chem.* **30** No 8, 1121 (2006).
3. R. Esteban, A.G. Borisov, P. Nordlander, J. Aizpurua, *Nat. Commun.* 3 (2012).
4. Noguez, *J. Phys. Chem. C* **111** No 10, 3806 (2007).
5. W. Schrof, S. Rozouvan, E. Van Keuren, D. Horn, J. Schmitt, G. Decher, *Adv. Mater.* **10** No 4, 338 (1998).
6. M.A. Garcia, *J. Phys. D. Appl. Phys.* **44** No 28 (2011).
7. V.R.A. Holm, M.M. Greve, B. Holst, *J. Vac. Sci. Technol. B* **34** No 6 (2016).
8. S. Rozouvan, *J. Opt. Soc. Am. B* **17** No 8, 1354 (2000).
9. S. Mossman, R. Lytel, M.G. Kuzyk, *J. Opt. Soc. Am. B* **33** No 12, E31 (2016).

Дисперсійні властивості нелінійності третього роду поверхневого плазмонного резонансу в золотих наночастинках

Л. Поперенко, С. Розуван, В. Стащук

Київський національний університет імені Тараса Шевченка, фізичний факультет,
проспект Глушкова, 4, Київ 03022, Україна

В роботі представлені експериментальні результати фемтосекундної чотирьохпучкової спектроскопії з полімерними напівпровідниковими плівками з золотими наночастинками, проведені в видимій області спектру. Було експериментально зареєстровано підсилення оптичної нелінійності третього роду на короткохвильовому крилі плазмонної полоси поглинання. Для аналізу експериментальних даних в роботі була розроблена теоретична модель поверхневих плазмонів як повздовжніх стоячих хвиль в нанооб'єктах. При цьому підсилення нелінійних коефіцієнтів третього роду відбувається в спектральній області з одночасно великими значеннями діелектричної проникності та коефіцієнта заломлення. Експерименти з застосуванням скануючої тунельної мікроскопії з просторовою роздільною здатністю до 1 нм дозволили детально охарактеризувати морфологію зразка з золотими наночастинками. Результати мікроскопії показали, що наночастинки розміром 10-20 нм мають несферичну форму та аморфне впорядкування атомів. При цьому наночастинки є згрупованими в кластери з розмірами до декількох сотень нанометрів. В роботі були отримані чисельні розв'язки рівнянь Максвела для наночастинок з формою поверхні експериментально зареєстрованою методикою скануючої тунельної мікроскопії. Результати обчислень підтверджують однорідний характер спектрального уширення плазмонної полоси поглинання в зразках і коректність представленого теоретичного підходу, при якому спектральні властивості поверхневого плазмону можуть розглядатися в моделі гармонічного осцилятора з затуханням. Чотирьохпучкова вироджена взаємодія в композитному матеріалі на основі органічного полімеру з золотими наночастинками є одночасним проявом двох процесів – квантовомеханічних процесів оптичної нелінійності третього роду та повздовжньої стоячої хвилі носіїв заряду, яка коректно описується у рамках класичної електродинаміки.

Ключові слова: Поверхневий плазмон, Золоті наночастинки, Органічний напівпровідник, Нелінійність третього роду, Скануюча тунельна мікроскопія.